Journal of Alloys and Compounds 509 (2011) 3651–3655

Contents lists available at ScienceDirect

Journal of Alloys and Compounds

journal homepage: www.elsevier.com/locate/jallcom

# $GdBaCo_2O_{5+\delta}$–$Sm_{0.2}Ce_{0.8}O_{1.9}$ composite cathodes for intermediate temperature SOFCs

Na Li[a], Bo Wei[a,*], Zhe Lü[a,*], Xiqiang Huang[a], Wenhui Su[a,b]

[a] Center for the Condensed Matter Science and Technology, Department of Physics, Harbin Institute of Technology, Harbin 150080, PR China
[b] International Center for Materials Physics, Academia Sinica, Shenyang 110015, PR China

ARTICLE INFO

*Article history:*
Received 18 August 2010
Received in revised form
15 December 2010
Accepted 17 December 2010
Available online 28 December 2010

*Keywords:*
Intermediate-temperature SOFC
Composite cathodes
$GdBaCo_2O_{5+\delta}$
Thermal expansion
Electrochemical performance

ABSTRACT

The $GdBaCo_2O_{5+\delta}$–$Sm_{0.2}Ce_{0.8}O_{1.9}$ (GBCO–SDC) composite cathodes were prepared, their thermogravimetric measurement, thermal expansion coefficient (TEC), electrical conductivity and electrochemical performance were studied as function of temperature and SDC content. The adjustment of TEC to electrolyte, which is one of the main problems of GBCO cathode, could be achieved to lower TEC values with more SDC addition, while maintaining reasonable high electrical conductivity. By means of DC polarization and AC impedance spectroscopy, the electrochemical performance of GBCO–SDC composite cathodes on SDC electrolyte was examined. Results indicated that the proper addition of SDC could improve the performance of GBCO cathode. The optimum content of SDC in the composite cathodes was 40 wt.% with the polarization resistance (Rp) of 1.39 $\Omega\,cm^2$ at 500 °C, which was significantly lower than that of pure GBCO cathode (7.26 $\Omega\,cm^2$).



## 1. Introduction

At present, intermediate-temperature (500–800 °C) SOFCs (IT-SOFCs) have been the main SOFC research object because the reduced operating temperature can extend the range of material selection for cell components, reduce cost of SOFC system and prolong the life of cells. However, traditional cathode materials, like $La_{1-x}Sr_xMnO_3$ (LSM), cannot provide satisfactory performance below 700 °C, and therefore much effort has been devoted to the development of new cathode materials for IT-SOFCs.

Double-perovskite structure cobaltites, such as $PrBaCo_2O_{5+\delta}$ (PBCO), $GdBaCo_2O_{5+\delta}$ (GBCO) and $SmBaCo_2O_{5+\delta}$ (SBCO) have been considered as promising cathode materials for IT-SOFCs. Because these materials have high oxide ionic diffusivity, rapid oxygen-transport and surface-exchange kinetics, which result in their excellent electrocatalytic behavior for oxygen reduction reaction even at reduced temperatures [1–3]. In our previous work, $GdBaCo_2O_{5+\delta}$ (GBCO) has been studied as a promising cathode material for IT-SOFCs. It showed high conductivity about 512–290 S $cm^{-1}$ in the temperature range of 500–800 °C, and had good chemical compatibility with $Sm_{0.2}Ce_{0.8}O_{1.9}$ (samaria-doped ceria, SDC) electrolyte. In addition, its electrochemical performance was better than many other cathode materials (such as SSC and LSC) under similar conditions [4,5]. However, similar to other Co-based materials [6], the thermal expansion coefficient (TEC) of GBCO ($\sim 20.1 \times 10^{-6}\,K^{-1}$) was too high to match with that of doped ceria electrolytes ($\sim 12 \times 10^{-6}\,K^{-1}$) [7,8]. The thermal expansion mismatch could induce that the cathode crack during thermal cycling, which is deleterious to the performance of SOFCs.

Normally, the thermal expansion mismatch could be adjusted by two methods: one way is doping ions with small ionic radius (such as Fe) at B-site (replacing Co) to reduce the TEC [9,10]. Another way is to add other materials with lower TEC into the cathode, such as electrolyte materials [11,12]. Dyck et al. [11] have pointed out that adding $Ce_{0.8}Gd_{0.2}O_{1.95}$ electrolyte to the $Gd_{0.8}Sr_{0.2}CoO_{3-\delta}$ cathode served to moderate the thermal expansion and resulted in excellent matching to the doped-ceria electrolyte material. For instance, even a 12.5 wt.% addition of $Ce_{0.8}Gd_{0.2}O_{1.95}$ obviously reduces the thermal expansion coefficient of the cathode from $23 \times 10^{-6}$ to $13.5 \times 10^{-6}\,K^{-1}$ over the same temperature range. Furthermore, the addition of electrolyte material (ionic conducting phase) also could improve the electro-catalytic performance of the cathodes. Several composite cathodes, like (La,Sr)$MnO_3$–$Ce_{0.8}Gd_{0.2}O_{2-\delta}$ and $La_{0.6}Sr_{0.4}Co_{0.2}Fe_{0.8}O_{3-\delta}$–$Ce_{0.9}Gd_{0.1}O_{2-\delta}$ have proven to exhibit higher electrochemical properties than pure cathodes. With 50 wt.% $Ce_{0.8}Gd_{0.2}O_{2-\delta}$ addition to (La,Sr)$MnO_3$ cathode, the polarization resistance decreased from 16.32 $\Omega\,cm^2$ (for pure LSM) to 4.44 $\Omega\,cm^2$ at 600 °C in air [13]; The optimum $Ce_{0.9}Gd_{0.1}O_{2-\delta}$ addition (36% by volume) to $La_{0.6}Sr_{0.4}Co_{0.2}Fe_{0.8}O_{3-\delta}$ resulted in four times lower area specific resistance [14–16]. These results classify

* Corresponding authors. Tel.: +86 451 8641 8420; fax: +86 451 8641 8420.
*E-mail addresses:* bowei@hit.edu.cn (B. Wei), lvzhe@hit.edu.cn (Z. Lü).

0925-8388/$ – see front matter © 2010 Elsevier B.V. All rights reserved.
doi:10.1016/j.jallcom.2010.12.147

composite cathodes as promising materials for IT-SOFC operation. Therefore, the composite cathode composed of $GdBaCo_2O_{5+\delta}$ (GBCO) cathode and $Sm_{0.2}Ce_{0.8}O_{1.9}$ (SDC) electrolyte is expected to bring better properties than pure GBCO as a cathode material in intermediate temperature range.

In this paper, the various GBCO–SDC*x* (*x* = 20, 30, 40, 50, 60 wt.%) composite cathodes were fabricated, their thermogravimetric measurement, thermal expansion coefficient, electrical conductivity and electrochemical performance were investigated.

## 2. Experimental

$GdBaCo_2O_{5+\delta}$ (GBCO) powders were prepared by the conventional solid-state reaction method as reported in previous paper [4]. $Sm_{0.2}Ce_{0.8}O_{1.9}$ (SDC) powders were prepared via citric acid assisted combustion method. Composite cathodes were prepared by adding SDC powders in amounts of 20, 30, 40, 50 and 60 wt.% to GBCO powders, named as GBCO–SDC*x* (*x* = 20, 30, 40, 50, and 60). These powders were ground thoroughly in ethanol using a mortar and pestle, followed by drying and dry grinding to produce uniform mixtures. The cathode slurries were prepared by grounding the GBCO and GBCO–SDC*x* powders mixed with ethyl cellulose and terpineol. Uniaxially pressed SDC electrolyte pellets were sintered at 1400 °C for 4 h in air. To improve the adhesion of interface, a SDC layer was spin coated onto the surface of SDC pellet before sintering.

For conductivity and thermal expansion tests, GBCO and GBCO–SDC*x* powders were pressed into dense disks and sintered at 1050 °C for 4 h in air, then cut into rectangular bars. The electrical conductivity was measured by a standard four-point method using a measuring system including Keithley 2400 digital source meter combined with an AI808P temperature controller. Four silver leads were attached to the GBCO–SDC bars with silver paste (DAD-87) to obtain good electrical contacts between the silver leads and the sample. A direct current was passed through the two outside leads, and the voltage was measured between the two inside leads. Thermal expansion coefficient (TEC) was measured using a Netzsch DIL 402C/3/G dilatometer from room temperature to 900 °C with air purge (flow rate is 50 ml/min). Thermogravimetric measurement was performed in air from room temperature to 1000 °C with a heating rate of 10 K/min.

For the measurements of electrochemical performances, these slurries of GBCO and GBCO–SDC*x* were painted on the one side of SDC pellets to form two electrodes, one as working electrode (≈0.2 $cm^2$ in area) and the other as reference electrode, then sintered at 1050 °C for 4 h. The counter electrode, which had the same shape, size and position as the working cathode, was made by painting the silver paste (DAD 87) on the other side of the electrolyte pellets. The electrochemical performances of GBCO and GBCO–SDC*x* composite cathodes on SDC electrolyte were characterized by impedance spectroscopy and polarization curves, which were carried our by an electrochemical interface (Solartron SI 1287) and a frequency response analyzer (Solartron SI 1260) in the temperature range of 500–800 °C. The AC impedance spectra were obtained under open circuit condition with a 10 mV AC signal in the frequency range of 0.1 Hz–91 kHz.

## 3. Results and discussion

### 3.1. Electrical conductivity

Fig. 1a shows the thermal gravimetric curves of pure GBCO and GBCO–SDC composite samples obtained in air. All curves were normalized based on the amount of GBCO in the composite. For pure GBCO, the loss of adsorbed water and other gases leads to a decrease in the weight of GBCO observed from room temperature to ~200 °C. After a heating–cooling cycle, this decrease of weight before ~200 °C was eliminated. From ~200 to ~300 °C, the weight of GBCO has slight increase with the increase of temperature, it may be caused by the oxidization of $Co^{3+}$ to $Co^{4+}$, in order to maintain electrical neutrality, the amount of oxygen vacancies lessen, accompanied by the increase of weight. The equilibrium given in Eq. (1) is shifted to the left [17,18].

$$2Co_{Co}^{\bullet}(IV) + O_O^{\times} \Leftrightarrow 2Co_{Co}^{\times}(III) + V_O^{\bullet\bullet} + \frac{1}{2}O_2 \quad (1)$$

In addition, the charge carrier (electron hole) concentration increases with the increasing $Co^{4+}$ ion, so the conductivity of GBCO increases with temperature before ~300 °C (as shown in Fig. 2).

After ~300 °C, the weight of GBCO starts to decrease with increasing temperature, it is attributed to the reduction of $Co^{4+}$ to $Co^{3+}$, which must occur concurrently with the creation of oxygen vacancies (reduction in oxygen content) to maintain electrical neutrality. At the same time, the oxidization of $Co^{3+}$ to $Co^{4+}$ is still in progress, this equilibrium is shifted to two-way, but chief between them is the reduction, so the total expression is oxygen loss (weight loss), and the concentration of electronic charge carriers decrease gradually with the decrease of $Co^{4+}$ ion, which result in

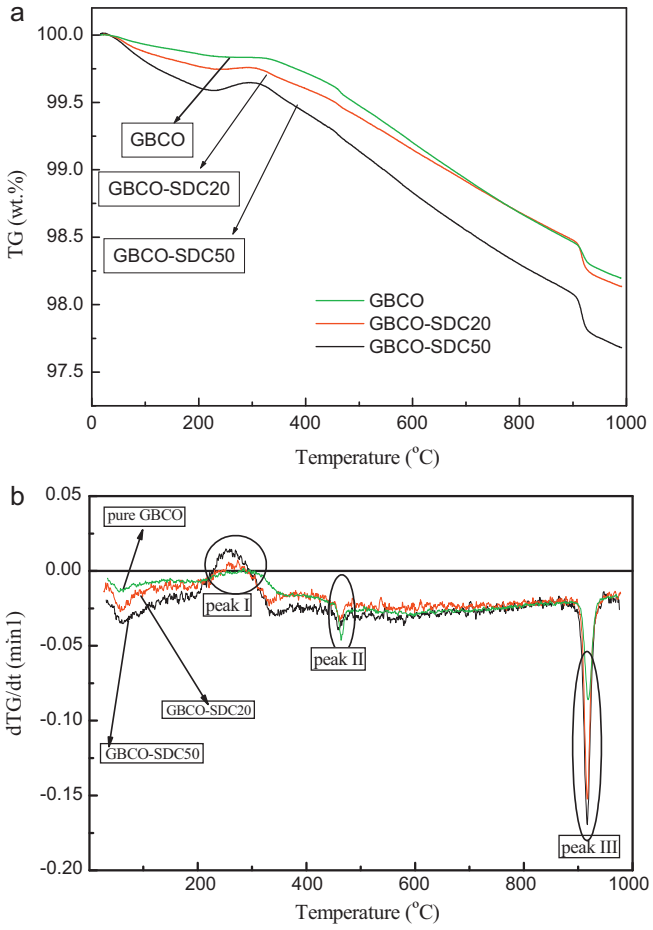


**Fig. 1.** (a) TG curves of pure GBCO and GBCO–SDC*x* composite measured in air at a heating temperature rate of 10 K/min. (b) First derivative of the thermogravimetric data versus time for pure GBCO and GBCO–SDC*x* composite.

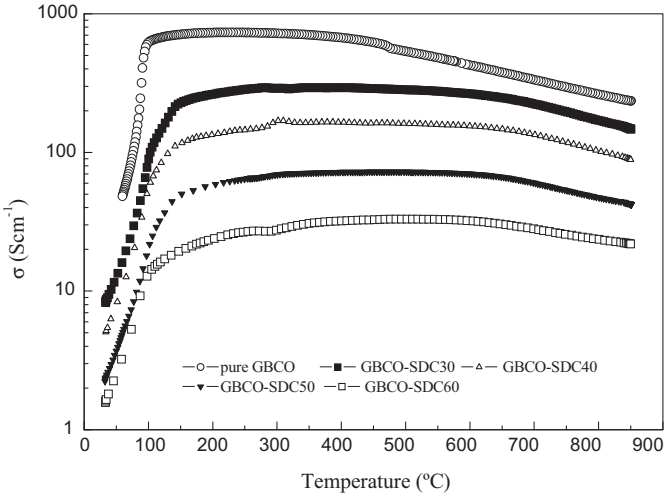


**Fig. 2.** Electrical conductivity as a function of temperature for the pure GBCO and GBCO–SDC*x* composite in air.

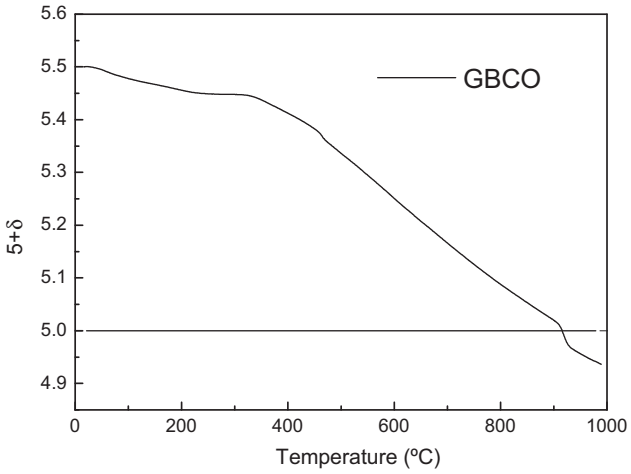


**Fig. 3.** Oxygen nonstoichiometry of $GdBaCo_2O_{5+\delta}$ as a function of temperature.

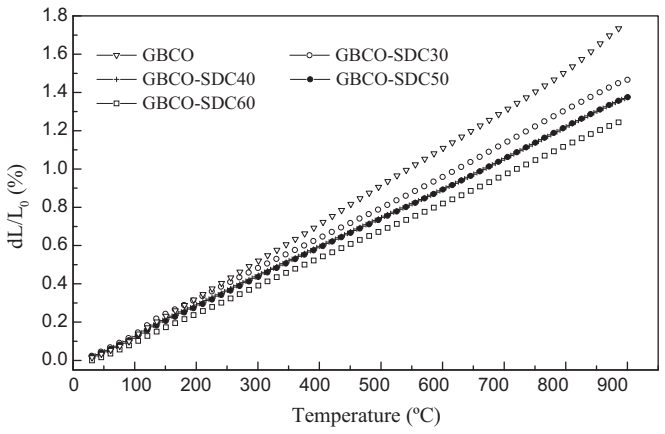


**Fig. 4.** Thermal expansion curves of pure GBCO and GBCO–SDC*x* composite samples.

the decrease in conductivity of GBCO after about 300 °C. At ~466 °C, it is observed that the TG curve has an abnormal decrease, it may be due to the end of oxidization, i.e. only the reduction of $Co^{4+}$ to $Co^{3+}$ happen, the process of assimilate oxygen do not exist, so the oxygen loss is more obvious than preceding stage. In addition, the decrease in electronic charge carriers concentration is more obvious, which cause that the slope of decrease in conductivity with the increase of temperature is steeper after the same onset temperature (~466 °C) (as shown in Fig. 2). Tarancon et al. reported that $GdBaCo_2O_{5+x}$ shows a phase transition from orthorhombic *Pmmm* to tetragonal *P4/mmm* at ca. 475–500 °C, and this transition is associated with the oxygen order–disorder phase transition [19]. In addition, according to Streule et al. [20], $PrBaCo_2O_{5.48}$ shows the orthorhombic–tetragonal phase transition at a similar temperature (503 °C), and a random redistribution of oxygen vacancies was observed across this temperature, which lead to an order–disorder transition. Thus, the inflection of TG curve for GBCO at ~466 °C could be accompanied by the same phase transition. In Fig. 1a, it yet is noticed that at about 917 °C, another abnormal decrease of TG curve occurs. Theoretically, the total weight loss of GBCO will be 1.57%, when $Co^{4+}$ in GBCO are completely reduced to $Co^{3+}$, whereas the total weight loss will be 3.14% if the complete reduction of $Co^{4+}$ to $Co^{2+}$. In experiment, the total weight loss of GBCO measured via TG curve was 1.63% at 917 °C, which indicated that parts of Co ion have been reduced to $Co^{2+}$. The reduction of $Co^{4+}$ to $Co^{2+}$ enhances the rate of oxygen loss, thereby resulting in the abnormal decrease of TG curve. Tsvetkov et al. reported that release of oxygen is accompanied by the formation of oxygen vacancies (associated with barium atoms) in the layers of $GdBaCo_2O_{6-}$ crystal lattice where they are ordered until the oxygen content achieves the value of 5.0 afterwards free oxygen vacancies are formed randomly elsewhere in oxygen polyhedrons [21]. As shown in Fig. 3, this temperature range of $T$ >917 °C corresponds to an oxygen content of $5+\delta<5.0$, therefore, there could be a transition from the formation of associated oxygen vacancies to that of free oxygen vacancies which took place at ~917 °C.

The similar change about weight is also observed for the GBCO–SDC*x* composite, but there is still some difference. The first derivative of the TG data (in Fig. 1a) is given out in Fig. 1b. The main three peaks were identified as the peak I, peak II and peak III, respectively. As can be seen, a apparent change in the position of the peak I and peak II was observed with an increase in SDC content, the SDC addition shifts the peak I and peak II towards lower temperature: the peak I appears at 276–297 °C for pure GBCO, at 274 °C for GBCO–SDC20, at 252 °C for GBCO–SDC50. The peak II appears at 464 °C for pure GBCO, at 460 °C and 458 °C for GBCO–SDC20 and GBCO–SDC50. The shift in position of peaks I, II can be attributed to the catalytic effect of SDC ($CeO_2$-based oxides) on the incorporation and release process of oxygen in GBCO–SDC*x* composite. However, there is almost no change observed in the position of peak III (at about 917 °C) with SDC addition, which may be because the temperature (>900 °C) is high enough to promote the oxygen diffusion and oxidation processes so that there is no need to depend on the SDC addition.

The temperature dependence of electrical conductivity for GBCO–SDC*x* composite materials are shown in Fig. 2. As can be seen, these materials have a similar temperature dependence. When the temperature is lower than 100 °C, the conductivity rapidly increases with temperature. Then the conductivity changes slowly above 100 °C, and exhibits a transition from semi-conductive to metallic behavior.

As expected, at all temperatures, the conductivity decreases with the increase of SDC addition in cathode. It is suggested that the higher addition of excellent ionic conducting phase SDC results in more interruptions in the GBCO matrix, which block the flow of electronic current. The specific conductivity values for the GBCO and GBCO–SDC*x* composite materials at various temperatures are listed in Table 1.

### 3.2. Thermal expansion

The thermal expansion curves of GBCO and GBCO–SDC composite samples sintered at 1050 °C are presented in Fig. 4. The averaged thermal expansion coefficient (TEC) values (between room temperature and 900 °C) calculated from these curves

**Table 1**
Specific conductivity values at various temperatures.

| | GBCO | GBCO–SDC30 | GBCO–SDC40 | GBCO–SDC50 | GBCO–SDC60 |
|---|---|---|---|---|---|
| 500 °C | 512 | 283 | 162 | 72 | 33 |
| 600 °C | 427 | 265 | 155 | 70 | 32 |
| 700 °C | 348 | 224 | 134 | 60 | 28 |
| 800 °C | 289 | 170 | 103 | 47 | 24 |

**Table 2**
The average TEC values in the temperature range of 30–900 °C.

| | GBCO | GBCO–SDC30 | GBCO–SDC40 | GBCO–SDC50 | GBCO–SDC60 |
|---|---|---|---|---|---|
| TEC ($K^{-1}$) | $20.10 \times 10^{-6}$ | $16.70 \times 10^{-6}$ | $15.63 \times 10^{-6}$ | $15.60 \times 10^{-6}$ | $14.60 \times 10^{-6}$ |

are listed in Table 2. As expected, the TEC for composite materials decreases with the increasing SDC content. The addition of SDC electrolyte moderates the TEC of the cathode and improves the thermal compatibility with the electrolyte. The same phenomena have been observed in $La_{0.6}Sr_{0.4}Co_{0.8}Fe_{0.2}O_{3-\delta}$–$Ce_{0.8}Sm_{0.2}O_{2-\delta}$, $Ba_{0.5}Sr_{0.5}Co_{0.6}Fe_{0.4}O_{3-\delta}$–$Ce_{0.8}Sm_{0.2}O_{1.9}$, $La_{0.7}Sr_{0.3}CuO_{3-\delta}$–$Sm_{0.2}Ce_{0.8}O_{2-\delta}$ composite [12,22,23]. It is considered that the TEC of GBCO–SDC composite is controlled mainly by the SDC phase, the adjacent SDC grains likely restrained the thermal expansion of GBCO grains.

### 3.3. Electrochemical performance

The overpotential, also called polarization, is an important factor imaging the performance of the electrode [24,25]. The lower cathodic overpotential represents the higher catalytic activity for oxygen reduction. Fig. 5 shows the polarization curves for GBCO and GBCO–SDC*x* composite cathodes at 500 and 600 °C with SDC as the electrolyte. From Fig. 5, it can be known that, under same current density, the overpotential decreased with increasing SDC content.

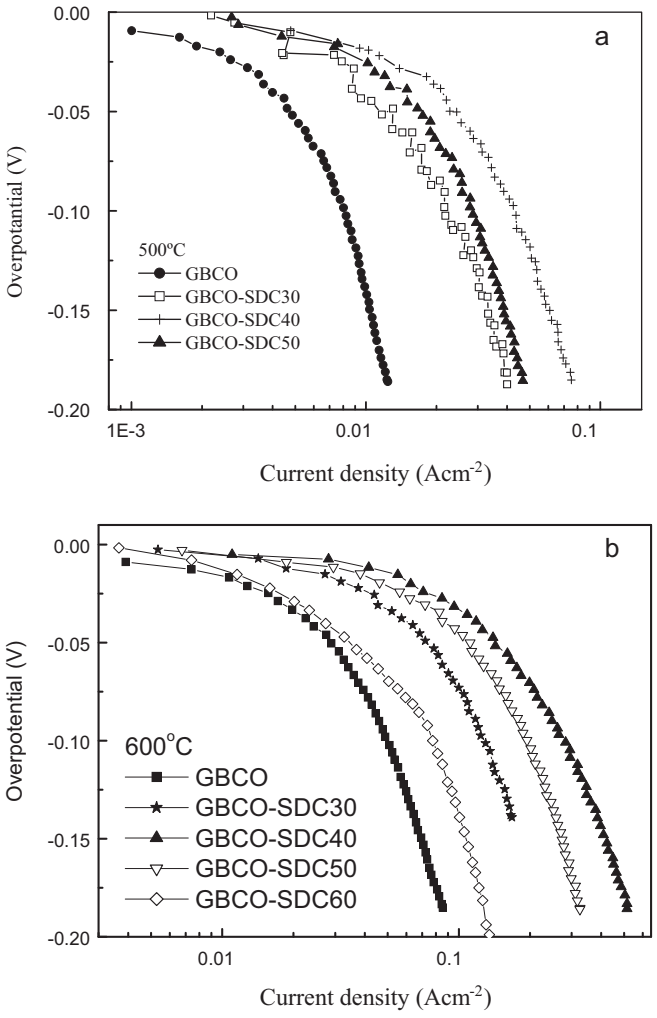


**Fig. 5.** Polarization curves for GBCO and GBCO–SDC*x* composite cathodes obtained at (a) 500 °C and (b) 600 °C.

When the amount of SDC reached to 40 wt.%, the lowest overpotential was obtained and then started increasing above 40 wt.%. This tendency was found at each temperature. Fig. 6(a) shows the half cell polarization resistances Rp (which obtained from fitting results using the Zview program) of different GBCO–SDC*x* composite cathodes as a function of SDC content measured at various temperatures. Fig. 6(b) shows Nyquist plots of half cells with GBCO and GBCO–SDC40 composite cathode at 600 °C. As expected, the GBCO–SDC40 composite exhibited the lowest polarization resistance at each temperature. Its Rp value was 1.39 Ω cm$^2$ at 500 °C, meanwhile the value was 7.26 Ω cm$^2$ for pure GBCO cathode. In addition, the performance of GBCO–SDC was better than many other composite cathodes at low temperature range, for example, $PrBaCo_2O_{5+\delta}$–$Ce_{0.8}Sm_{0.2}O_{1.9}$ composite cathode [26]. Fig. 7 shows the Arrhenius plots of the polarization resistance of pure GBCO and GBCO–SDC composite cathodes. The activation energy can be calcu-

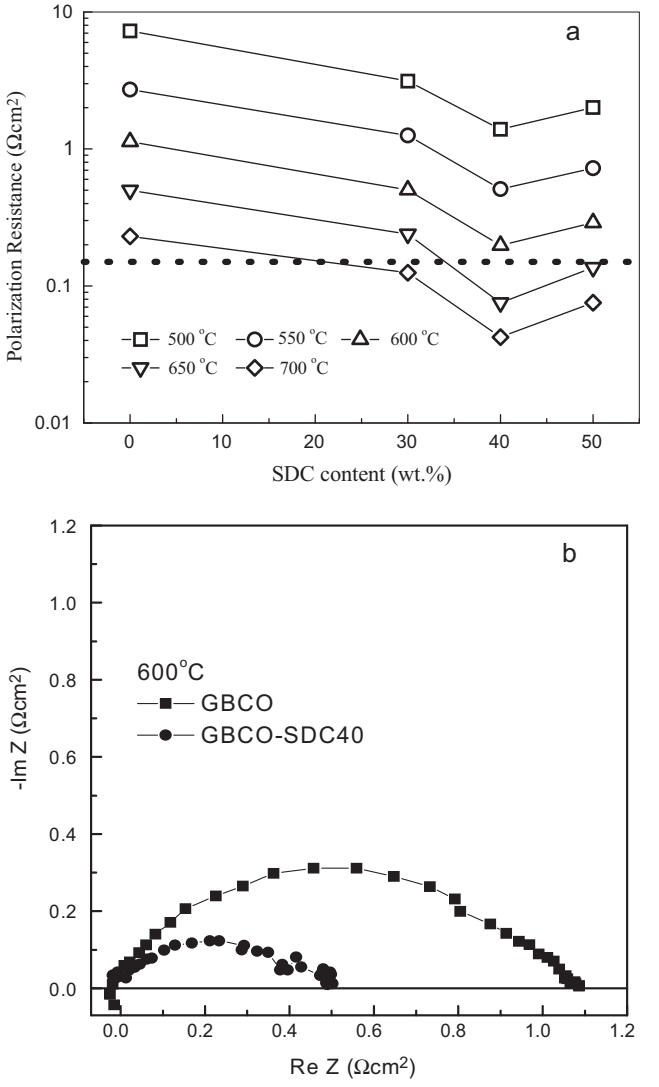


**Fig. 6.** (a) Plot of the half cell polarization resistance versus SDC contents at different temperatures, the dot line represents Rp = 0.15 Ω cm$^2$. (b) Nyquist plots of half cells with GBCO and GBCO–SDC40 composite cathode at 600 °C.

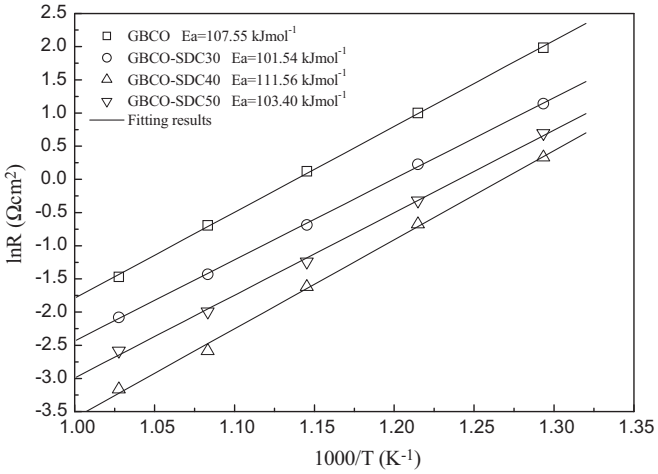


**Fig. 7.** Arrhenius plots of the polarization resistance of GBCO and GBCO–SDC*x* cathodes.

lated from the slope of the fitted line. The activation energy values on the four samples are close (all in the range of $107 \pm 5\,kJ\,mol^{-1}$). This indicates that the SDC addition may not change the rate-limiting mechanism for the cathode reaction process.

The electrochemical characteristics of GBCO–SDC composites suggest that SDC play an important role in enhancing the performance of cathode. The observed higher catalytic activity of GBCO–SDC composite cathodes than pure GBCO might be due to the addition of SDC electrolyte extends the triple phase boundary (TPB) further into the cathodes, which caused the lower overpotential [27]. In addition, the addition of ionic conducting phase SDC would increase oxygen diffusion, and the SDC/SDC interface at the GBCO–SDC/SDC interface is an easier path for oxygen ionic transport than GBCO/SDC interface. However, the performance decreased for further increasing SDC content above 40 wt.%. The cause may be that too much SDC electrolyte decreased the continuity of the GBCO in the composite, thereby resulting in a decrease in electrical conductivity and electrochemical properties.

## 4. Conclusions

The GBCO–SDC composite cathodes were prepared and studied for potential applications in intermediate-temperature SOFCs. The thermogravimetric data of pure GBCO and GBCO–SDC composite indicated the SDC addition expedited the incorporation and release process of oxygen in GBCO–SDC*x* composite. The thermal expansion results of GBCO–SDC composite cathodes indicated that SDC addition reduced the TEC of composite cathodes and improved the thermal expansion match between the electrolyte and the cathode. Even though the SDC addition decreased the electrical conductivity of cathode, the GBCO–SDC*x* composites for $x \leq 40$ wt.% still reached the electrical conductivity requirement ($\geq 100\,S\,cm^{-1}$) for a cathode material of IT-SOFC. The effect of temperature and SDC content on electrochemical performance of cathode was studied by means of DC polarization and AC impedance spectroscopy using SDC as electrolyte. It was discovered that adding SDC electrolyte into GBCO cathode improved the performance of cathode. The optimum composite was GBCO–SDC40, which had the lowest overpotential or the smallest polarization resistance in the measured temperature range, its Rp was about $1.39\,\Omega\,cm^2$ at 500 °C, the value was ~5 times lower than that of pure GBCO. Therefore, this GBCO–SDC composite cathode should be a promising cathode material for IT-SOFCs based on SDC electrolytes.

## Acknowledgments

This work was supported by the Natural Science Foundation of China (20901020) and the Ministry of Science and Technology of China (2007AA05Z139).

## References

[1] G. Kim, S. Wang, A.J. Jacobson, L. Reimus, P. Brodersen, C.A. Mims, J. Mater. Chem. 17 (2007) 2500–2505.
[2] A.A. Taskin, A.N. Lavrov, Y. Ando, Appl. Phys. Lett. 86 (2005), 091910-1-3.
[3] A. Tarancón, A. Morata, G. Dezanneau, S.J. Skinner, J.A. Kilner, S. Estrade, F. Hernández-Ramírez, F. Peiró, J.R. Morante, J. Power Sources 174 (2007) 255–263.
[4] N. Li, Z. Lu, B. Wei, X.Q. Huang, K.F. Chen, Y.H. Zhang, W.H. Su, J. Alloys Compd. 454 (2008) 274–279.
[5] C.R. Xia, W. Rauch, F.L. Chen, M.L. Liu, Solid State Ionics 149 (2002) 11–19.
[6] H.Y. Tu, Y. Takeda, N. Imanishi, O. Yamamoto, Solid State Ionics 100 (1997) 283–288.
[7] E.Yu. Pikalova, V.I. Maragou, A.N. Demina, A.K. Demin, P.E. Tsiakaras, J. Power Sources 181 (2008) 199–206.
[8] H. Hayashi, M. Kanoh, C.J. Quan, H. Inaba, S. Wang, M. Dokiya, H. Tagawa, Solid State Ionics 132 (2000) 227–233.
[9] H. Lv, Y.J. Wu, B. Huang, B.Y. Zhao, K.A. Hu, Solid State Ionics 177 (2006) 901–906.
[10] L.-W. Tai, M.M. Nasrallah, H.U. Anderson, D.M. Sparlin, S.R. Sehlin, Solid State Ionics 76 (1995) 259–271.
[11] C.R. Dyck, Z.B. Yu, V.D. Krstic, Solid State Ionics 171 (2004) 17–23.
[12] Q. Xu, D.P. Huang, F. Zhang, W. Chen, M. Chen, H.X. Liu, J. Alloys Compd. 454 (2008) 460–465.
[13] E.P. Murray, S.A. Barnett, Solid State Ionics 143 (2001) 265–273.
[14] V. Dusastre, J.A. Kilner, Solid State Ionics 126 (1999) 163–174.
[15] H.J. Hwang, J.W. Moon, S.H. Lee, E.A. Lee, J. Power Sources 145 (2005) 243–248.
[16] E.P. Murray, M.J. Sever, S.A. Barnett, Solid State Ionics 148 (2002) 27–34.
[17] B. Wei, Z. Lü, S.Y. Li, Y.Q. Liu, K.Y. Liu, W.H. Su, Electrochem. Solid-State Lett. 8 (2005) A428–A431.
[18] S.Y. Li, Z. Lü, X.Q. Huang, B. Wei, W.H. Su, Solid State Ionics 178 (2007) 417–422.
[19] A. Tarancon, D. Marrero-Lopez, J. Pena-Martinez, J.C. Ruiz-Morales, P. Nunez, Solid State Ionics 179 (2008) 611–618.
[20] S. Streule, A. Podlesnyak, D. Sheptyakov, E. Pomjakushina, M. Stingaciu, K. Conder, M. Medarde, M.V. Patrakeev, I.A. Leonidov, V.L. Kozhevnikov, J. Mesot, Phys. Rev. B 73, 094203 (2006).
[21] D.S. Tsvetkov, V.V. Sereda, A.Yu. Zuev, Solid State Ionics 180 (2010) 1620–1625.
[22] S.Y. Li, Z. Lü, B. Wei, X.Q. Huang, J.P. Miao, Z.G. Liu, W.H. Su, J. Alloys Compd. 448 (2008) 116–121.
[23] X.F. Ding, C. Cui, L.C. Guo, J. Alloys Compd. 481 (2009) 845–850.
[24] J.D. Zhang, Y. Ji, H.B. Gao, T.M. He, J. Liu, J. Alloys Compd. 395 (2005) 322–325.
[25] X.Q. Huang, L. Pei, Z.G. Liu, Z. Lv, Y. Sui, Z.N. Qian, W.H. Su, J. Alloys Compd. 345 (2002) 265–270.
[26] C.J. Zhu, X.M. Liu, C.S. Yi, L. Pei, D.J. Wang, D.T. Yan, K.G. Yao, T.Q. Lü, W.H. Su, J. Power Sources 195 (2010) 3504–3507.
[27] H. Fukunaga, M. Ihara, K. Sakaki, K. Yamada, Solid State Ionics 86–88 (1996) 1179–1185.